** This is the accepted version of the paper published in: 2024 IEEE 37th International Conference on Micro Electro Mechanical Systems (MEMS), Austin, TX, USA, 2024, pp. 745-748, https://doi.org/10.1109/MEMS58180.2024.10439404

ENHANCING POWER DENSITY THROUGH ELECTRODE CONFIGURATION FOR PIEZOMEMS ENERGY HARVESTER

Ranjith Janardhana[1], Sean Smith[3], Naomi Montross[3], Joe Evans[3], and Nathan Jackson[1,2]
[1]Mechanical Engineering Department University of New Mexico, USA
[2] Nanoscience & Microsystems Engineering University of New Mexico, USA
[3]Radiant Technologies, USA

ABSTRACT

Microelectromechanical Systems (MEMS) energy harvesters have been extensively investigated over the past decade, but increasing power density and long-term reliability under high acceleration and low frequency are still major concerns. This study focused on the development of a low-frequency lead zirconate titanate (PZT) based energy harvester capable of operating at high acceleration >4 g with high power density performance. This study investigates the performance effects of altering the electrode configuration and poling configuration to maximize power density. The study investigated using four different types of electrode configuration consisting of long and short electrodes with interdigitated electrodes (IDE) to operate in d_{33} mode, and traditional parallel plate configuration to operate in d_{31} mode. The results were numerically and experimentally validated. The results illustrate that the d_{33} mode configuration was able to generate >3200 μW mm^{-3} with good reliability of up to 4 g.

KEYWORDS

Lead Zirconate Titanate, Piezoelectric, Energy Harvester, d_{33}, MEMS.

INTRODUCTION

Recently there has been an extensive amount of research focused on developing PiezoMEMS energy harvesting devices for various applications from IoT to biomedical [1-3]. However, there are still major challenges that need to be resolved before these can be commercialized including 1) increasing power density, 2) increasing bandwidth, 3) tuning the resonant frequency, and 4) long-term reliability. Increasing power density along with decreasing power requirements from electronics is necessary to create a self-sustaining system. Power density is a major issue for MEMS devices as power generation decreases exponentially as devices are scaled down, and there is a demand for devices to be smaller in order to decrease the footprint of the entire system.

Several methods of increasing power density have been investigated including optimization of piezoelectric materials, optimization of the shape of the cantilever, and recently optimization of electrode configuration. Thin film piezoelectric materials commonly used in MEMS energy harvesters include Aluminum nitride (AlN) and its alloys, Zinc Oxide (ZnO), and lead zirconate titanate (PZT). AlN and ScAlN based devices have demonstrated higher power density than PZT and ZnO when using similar thicknesses and layers, due to its low dielectric properties and high elastic modulus [4-8]. However, ZnO and AlN are non-ferroelectric, which means they cannot be poled to alter their orientation after deposition. Researchers have also had success at altering the shape of the energy harvester in order to maximize stress distribution [9, 10]. Other attempts to increase power density include applying external forces such as magnetics to alter the acceleration of the cantilever beam [11, 12].

Previous attempts have been investigated to alter the electrode configuration while using ferroelectric-based piezoelectric materials to alter the poling orientation of the film. Initial work has demonstrated that interdigitated electrodes (IDE) can be used to pole the PZT film so that the stress/strain and voltage potential are in the same orientation thus allowing the device to operate in the d_{33} mode. Typical piezoelectric films are poled or have orientation in the out-of-plane direction normal to the film, but the stress/strain occurs in the direction along the length of the cantilever thus resulting in operation in the d_{31} mode. The d_{33} properties of any piezoelectric film are larger (approximately 2x) than the value of d_{31}. Since the power generated is a function of piezoelectric properties, operating in the d_{33} mode should increase the voltage/power response.

The goal of this paper is to develop a low frequency PZT-based MEMS energy harvester and investigate the impact of varying electrode configuration on device performance. We investigated both IDE and parallel plate designs as well as electrode length. The material properties used to create the devices and their dimensions were kept constant. The performance was experimentally and numerically validated. The findings illustrate that the IDE electrode configuration gave a significant power density increase compared to parallel plate design and increasing the length of the electrodes resulted in increased power. The results demonstrate the successful development of a low frequency piezoMEMS energy harvesting with high power density with good reliability at low or high acceleration (>4 g)

MATERIALS AND METHODS

Concept

The concept of using IDE electrodes to operate in the d_{33} mode has been previously documented through computational analysis [13-16]. The overall concept can be viewed in Figure 1.

The traditional electrode configuration is a parallel plate configuration consisting of a top and bottom electrode and a piezoelectric material between them. Poling of ferroelectric material results in the films domains being oriented in the direction normal to the electrodes. However, as the cantilever oscillates the stress/strain produced is along the length of the cantilever, which results in a d_{31} mode of operation. On the other hand, poling the

piezoelectric material using an IDE configuration, results in the piezoelectric materials domains to be oriented along the length of the cantilever to essentially operate in the d_{33} mode. The spacing and dimensions of the IDE fingers are also significant and have been previously investigated through finite element modelling (FEM) [17].

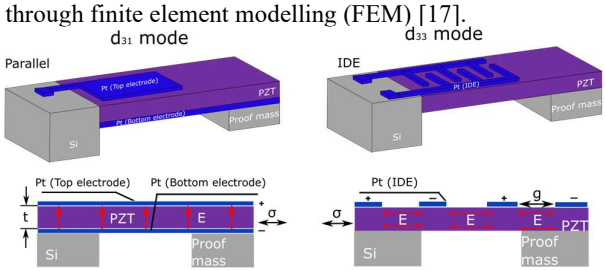

Figure 1: Schematic illustrating the two types of electrode configurations and their cross-section image showing the poling and orientation to operate in d_{31} or d_{33}mode.

Device Fabrication

The MEMS devices were fabricated using Radiant Technologies piezoMEMS foundry. Devices were fabricated on a 150 mm Si wafer and the stacked films used to create the device along with thickness values are shown in Figure 2. Briefly, the fabrication process consisted of growing a SiO_2 layer, followed by deposition and patterning of TiO_2/Pt which was used as the bottom electrode in the parallel plate configuration and used to grow the PZT film in the IDE configuration. Then PZT (52/48) was deposited using sol-gel techniques to a thickness of 1 µm. Next a top Pt electrode was deposited using e-beam deposition as the top electrode. In the case of the IDE, the top Pt electrode was patterned to meet IDE design requirements. A layer of PZT (20/80) was deposited as a protective layer followed by TiO_2 and spin on SiO_2 as insulating layers. A thick Cu layer was deposited to aid in stress relief and protection. The cantilever device was then released using deep reactive ion etching (DRIE) of the silicon and a proof mass of silicon (675 µm) was used to lower the frequency. The overall dimensions of the device were (1.3 x 0.58 x 0.0042 mm), length, width, and thickness respectively. Two different electrode lengths were developed (350 µm (short) and 900 µm (long)). The overall cantilever layers consisted of (SiO_2/TiO_2/Pt, PZT (52/48)/Pt/PZT (20/80)/SiO_2/Cu). The PZT films were poled by applying an electric field between the electrodes.

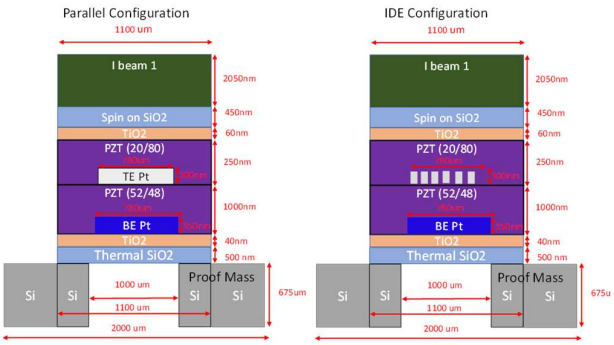

Figure 2: Cross section schematic of the various stacked layers in the piezoMEMS device.

Material Characterization

The various materials used in the device were characterized for average thickness using a scanning electron microscope (SEM). The elastic modulus of the films were characterized using nanoindentation [18], which was necessary for the FEM model and estimating the resonant frequency of the films. The piezoelectric properties were measured using a piezometer.

Numerical Simulations

COMSOL Multiphysics software was used to perform the FEM analysis of the device performance to compare the results to the experimental data. The FEM analysis was previously described in detail [17]. The main objective for the FEM analysis was to determine voltage output for IDE and parallel plate designs to determine if IDE does result in higher output due to the d_{33} mode of operation. The mechanical, electrical, and piezoelectric properties of the films were inserted into the model for increased accuracy. A 3D model was simulated at various accelerations and the voltage output was determined.

Experimental Characterization

After the devices were fabricated, they were diced and bonded upside down (proof mass facing up) onto a custom-made printed circuit board (PCB) as shown in Figure 4. The PCB was then mounted on a breadboard. The entire device was then attached to a vibration shaker (Labworks) which allowed us to control frequency and acceleration. The bandwidth and resonant frequency were determined by applying a frequency sweep and measuring voltage output. Voltage was measured using an oscilloscope and power was determined through a variable resistor which the impedance was set to match the impedance of the piezoMEMS device.

RESULTS AND DISCUSSION

The material characterization results are shown in Figure 3. The elastic modulus results are similar to previous values reported for each film. The piezoelectric properties of PZT (52/48) were: 90 pm V^{-1} for clamped film or d_{33} of 270 pm V^{-1} for free standing films. The values were averaged over several films and the values were consistently independent of their location on the wafer.

Layer # (Bottom->Top)	Measured Thickness (µm)	Modulus (GPa)
Silicon Dioxide	485	72
Titanium Dioxide	0.06	105
Platinum BE (e-beam)	0.16	138
FE		
PZT 52/48	0.98	147
PNZT 20/80	0.209	136
Platinum TE (e-beam)	0.1	168
Passivation		
SOG	0.536	50
I-Beam (e-beam Cu)	1.89	106

Figure 3: Results of material characterization of the layers used to make up the piezoMEMS device.

Figure 4 illustrates the design and fabrication of the four different devices. The cantilever dimensions and thickness of the layers were kept constant. The figure

shows the design of the IDE and parallel plate as well as the long and short version. The images illustrate the fabrication of the device, and the backside image shows the IDE electrode configuration. The bottom right image shows the device bonded to the PCB for testing.

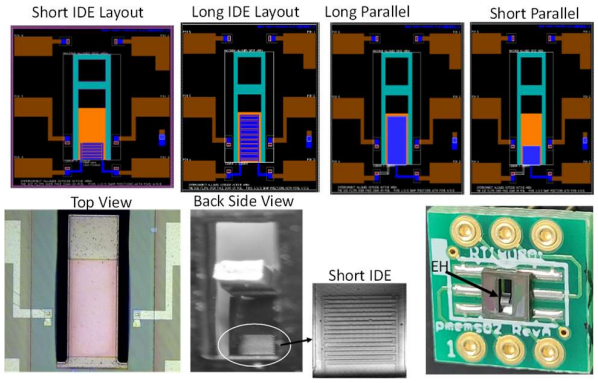

Figure 4: Top (schematic design of the four different electrode configurations investigated), bottom fabricated devices from different views.

The 3D FEM analysis results are illustrated in Figure 5. The results demonstrate that the IDE design resulted in higher voltage output compared to the parallel plate design across all accelerations up to 1 g. All simulations were operated at resonant frequency. The results illustrate that as acceleration increases the voltage difference between the two electrode configurations increases illustrating that the IDE d_{33} mode has better performance.

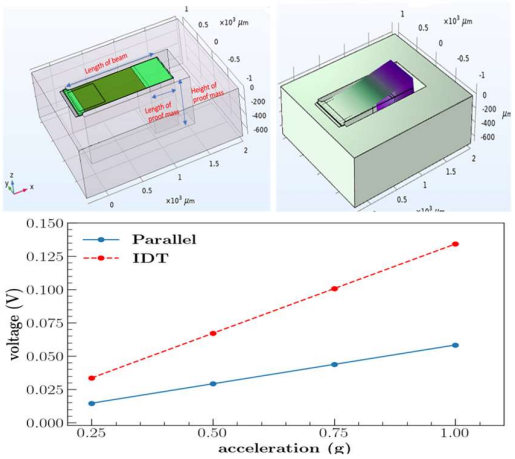

Figure 5: FEM analysis comparing the voltage output of IDE and parallel plate devices as a function of acceleration.

The resonant frequency, bandwidth and Q-factor can significantly influence the output voltage/power. Therefore, to systematically compare the various electrode configurations these properties should be similar. A laser interferometry system (SmartAct) was used to determine the displacement as a function of frequency with a low acceleration of 0.1 g. The results are shown in figure 6. The 1st mode resonant frequency of the four devices were 199.4 Hz, 198 Hz, 197.2 Hz, and 196.2 Hz for (long parallel, short IDE, Long IDE, and short parallel respectively). All devices had a similar resonant frequency within 3.2 Hz of each other. The slight variation is due to various mass differences in the different designs as well as slight differences in dimensions during fabrication. The displacement amplitudes were within 1 µm of each other for the same applied acceleration. The bandwidths were calculated from the full-width-half-maximum (FWHM) values which were 1.64, 1.46, 1.68, and 1.77 for the long IDE, short parallel, long parallel, and short IDE respectively. Therefore, mechanically speaking the four devices had similar properties including the Q-factor.

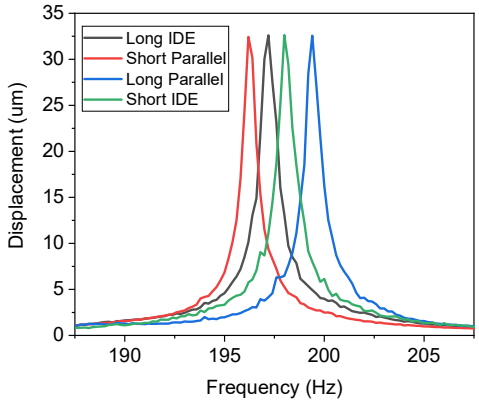

Figure 6: Experimental results of displacement as a function of frequency for the four devices.

The experimental results for power and power density as a function of acceleration are given in Figure 7. All measurements were performed at the resonant frequency. The results show that the long IDE design had the highest power compared to the other designs. Both IDE configurations had higher values than the parallel designs, and both long designs were significantly higher than the short designs. This agrees with the FEM model results. The power values saturated at 2 g, which is likely due to the cantilever having a large displacement causing it to impact the PCB, which saturated the peak power. Although this saturation limited output power it allowed the device to operate at high acceleration > 4 g. Long-term reliability was not performed but the device maintained its power for weeks with little deviation. The results demonstrate a new piezoMEMS energy harvesting device that can operate at low frequency, high acceleration, and maintain high power density.

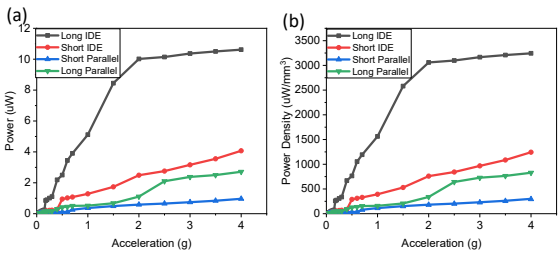

Figure 7: Experimental results of all four devices in terms of (a) power and (b) power density as a function of acceleration.

CONCLUSIONS

This study systematically compared micro-scale piezoMEMS energy harvesting devices with four different electrode configurations. The mechanical properties and dimensions of the devices were similar. The power results illustrate that the IDE configuration gave significantly higher power performance which agreed with previous results and 3D FEM simulations. The increased performance is believed to be due to the polarity of the PZT film allowing the device to operate in the higher order d_{33} mode. Although AlN based energy harvesters have demonstrated the potential to increase power density compared to PZT when both operated in d_{31} mode, the capability of PZT to be poled gives a potential advantage to enhance performance.

ACKNOWLEDGEMENTS

The authors would like to thank Radiant Technologies. The research was partially sponsored by the Defense Advanced Research Project Agency (DARPA) and was accomplished under Grant Number HR00121C0185. Part of the work was performed at the Center for Integrated Nanotechnologies, an Office of Science user Facility operated for the U.S. Department of Energy (DOE) under contract (89233218CNA0000001) and the NSF CAREER program grant number 2237086.

REFERENCES

[1] H. Ghoddus and Z. Kordrostami, "Harvesting the ultimate electrical power from mems piezoelectric vibration energy harvesters: an optimization approach," *IEEE Sensors Journal,* vol. 18, no. 21, pp. 8667-8675, 2018.

[2] O. Z. Olszewski, R. Houlihan, A. Blake, A. Mathewson, and N. Jackson, "Evaluation of vibrational PiezoMEMS harvester that scavenges energy from a magnetic field surrounding an AC current-carrying wire," *Journal of Microelectromechanical Systems,* vol. 26, no. 6, pp. 1298-1305, 2017.

[3] N. Jackson, O. Z. Olszewski, C. O'Murchu, and A. Mathewson, "Ultralow-frequency PiezoMEMS energy harvester using thin-film silicon and parylene substrates," *Journal of Micro/Nanolithography, MEMS, and MOEMS,* vol. 17, no. 1, pp. 015005-015005, 2018.

[4] R. Andosca *et al.*, "Experimental and theoretical studies on MEMS piezoelectric vibrational energy harvesters with mass loading," *Sensors and Actuators A: Physical,* vol. 178, pp. 76-87, 2012.

[5] S. S. Chauhan, M. M. Joglekar, and S. K. Manhas, "High power density CMOS compatible micro-machined MEMs energy harvester," *IEEE Sensors Journal,* vol. 19, no. 20, pp. 9122-9130, 2019.

[6] N. Jackson, R. O'Keeffe, F. Waldron, M. O'Neill, and A. Mathewson, "Evaluation of low-acceleration MEMS piezoelectric energy harvesting devices," *Microsystem technologies,* vol. 20, no. 4, pp. 671-680, 2014.

[7] N. Jackson, O. Z. Olszewski, C. O'Murchu, and A. Mathewson, "Shock-induced aluminum nitride based MEMS energy harvester to power a leadless pacemaker," *Sensors and Actuators A: Physical,* vol. 264, pp. 212-218, 2017.

[8] P. Mayrhofer *et al.*, "ScAlN MEMS cantilevers for vibrational energy harvesting purposes," *Journal of Microelectromechanical Systems,* vol. 26, no. 1, pp. 102-112, 2016.

[9] A. Nisanth, K. Suja, and V. Seena, "Design and optimization of MEMS piezoelectric energy harvester for low frequency applications," *Microsystem Technologies,* vol. 27, no. 1, pp. 251-261, 2021.

[10] G. Zhang, S. Gao, H. Liu, and S. Niu, "A low frequency piezoelectric energy harvester with trapezoidal cantilever beam: theory and experiment," *Microsystem Technologies,* vol. 23, pp. 3457-3466, 2017.

[11] M. Han, Q. Yuan, X. Sun, and H. Zhang, "Design and fabrication of integrated magnetic MEMS energy harvester for low frequency applications," *Journal of Microelectromechanical Systems,* vol. 23, no. 1, pp. 204-212, 2013.

[12] N. Jackson, "PiezoMEMS Nonlinear Low Acceleration Energy Harvester with an Embedded Permanent Magnet," *Micromachines,* vol. 11, no. 5, p. 500, 2020.

[13] N. Chidambaram, A. Mazzalai, D. Balma, and P. Muralt, "Comparison of lead zirconate titanate thin films for microelectromechanical energy harvester with interdigitated and parallel plate electrodes," *IEEE transactions on ultrasonics, ferroelectrics, and frequency control,* vol. 60, no. 8, pp. 1564-1571, 2013.

[14] S.-B. Kim, H. Park, S.-H. Kim, H. C. Wikle, J.-H. Park, and D.-J. Kim, "Comparison of MEMS PZT cantilevers based on $ d_ {31} $ and $ d_ {33} $ modes for vibration energy harvesting," *Journal of microelectromechanical systems,* vol. 22, no. 1, pp. 26-33, 2012.

[15] G. Tang, B. Yang, J.-q. Liu, B. Xu, H.-y. Zhu, and C.-s. Yang, "Development of high performance piezoelectric d33 mode MEMS vibration energy harvester based on PMN-PT single crystal thick film," *Sensors and Actuators A: Physical,* vol. 205, pp. 150-155, 2014.

[16] J. C. Park, J. Y. Park, and Y.-P. Lee, "Modeling and characterization of piezoelectric $ d_ {33} $-mode MEMS energy harvester," *Journal of Microelectromechanical Systems,* vol. 19, no. 5, pp. 1215-1222, 2010.

[17] R. D. Janardhana and N. Jackson, "COMPARATIVE ELECTRODE DESIGN FOR PIEZOELECTRIC MEMS KINETIC ENERGY HARVESTER," presented at the ASME International Mechanical Engineering Congress and Expostiion, New Orleans, 2023.

[18] P. Sharma, Z. Guler, and N. Jackson, "Development and characterization of confocal sputtered piezoelectric zinc oxide thin film," Vacuum, vol. 184, p. 109930, 2021.